Research Article | Vol. 30, No. 11 / 23 May 2022 / Optics Express 19990
Optics EXPRESS

# Laser source frequency drift compensation in Φ-OTDR systems using multiple probe frequencies

MOHAMMADMASOUD ZABIHI* AND KATERINA KREBBER

*Bundesanstalt für Materialforschung und -Prüfung, Unter den Eichen 87, 12205 Berlin, Germany*
*masoud.zabihi@bam.de

**Abstract:** Fully distributed fiber sensors, such as phase sensitive optical time domain reflectometry (Φ-OTDR) systems, have drawn significant attention from researchers, especially for use in geophysical applications. Distributed sensing, cost efficiency, wide dynamic range, good spatial resolution, and high accuracy make these sensors ideal for industrial use and for replacing traditional geophones. However, inevitable drifts in the central frequency of laser sources always cause low frequency noise in the output, which could easily be mistaken with real sub-Hertz environmental vibrations. This deteriorates the data accuracy, especially when dealing with low frequency seismic waves. In this study, we propose a method in which adding an extra probe frequency to a Φ-OTDR setup provides a reference frequency. This reference frequency provides information regarding changes in the laser source and other environmental noises, such as humidity and temperature, helping to refine extracted results from low frequency noise. This feature is also very useful for frequency domain analysis, where we may lose the near DC band information during mathematical measurements. Regarding the adjustable properties of this reference frequency, it can be implemented in various Φ-OTDR applications and commercial devices.



## 1. Introduction

Distributed acoustic sensors (DAS) have numerous applications in seismology, oil well monitoring, intrusion detection, and structural health monitoring [1–5]. One of the most important types of DAS is phase sensitive optical time domain reflectometry (Φ-OTDR). Φ-OTDR systems benefit from a long sensing range, suitable spatial resolution, fast response, and stability [6]. Φ-OTDR uses the coherent effect of Rayleigh backscattering (RBS) to sense and measure an external perturbation. A local disturbance on the sensing fiber causes elongation in fiber length and, consequently, a change in the optical path [6] that changes the phase of the received RBS. Another factor that influences the phase of each point on the fiber is the frequency of the probing light. Light source frequency drifting (LSFD) directly impacts the phase result at the output. Even the best laser sources available today on the market have slowly changing frequency drifts. Since these small frequency drifts can be easily misunderstood as external perturbations, they make Φ-OTDR systems unfit for low frequency detection, seismic applications, etc.

F. Zhu et al. [7] suggested a quasi-static measurement method to mitigate trace-by-trace distortion through laser frequency sweeping and cross-correlation measurement. This method is useful when working on sub-hertz level vibrations and when the pulse repetition rate is not high. Some differential methods have also been proposed to suppress LSFD by measuring the phase between two points and performing the measurement along the fiber under test (FUT) [8]. However, selecting the appropriate distance between two points is tricky and could be misleading in many applications, such as reservoir exploration. Q. Yuan [9] proposed a method using an auxiliary Mach–Zehnder interferometer. In that study the interferometer environment is different from the FUT, so the output may not resemble the behavior of the probe pulse in the FUT.

#460302 https://doi.org/10.1364/OE.460302
Journal © 2022 Received 4 Apr 2022; revised 27 Apr 2022; accepted 30 Apr 2022; published 19 May 2022

Optics EXPRESS

Xin et al. [10] also proposed a method based on an auxiliary Mach–Zehnder interferometer to mitigate phase jumps caused by the fading effect. In another study, a dual differential method was proposed that compared the two sides of the vibration area with another section of the FUT [11]. Although the system speed was acceptable, the selection of the reference section required further discussion. In another work [12], two sections were considered references and a differential measurement was performed. However, the applicability of this system when the vibration area is very long (e.g., in seismology) was not studied.

In this paper we propose a method that significantly removes the impact of LSFD in Φ-OTDR. The FUT carries two or more pulses with different frequencies, almost at the same time, and a comparison is made between the pulses. Use of multiple probe frequencies not only compensates LSFD in the measurement area (also known as the gauge length) but can suppress fading noise [13] at the same time with fast linear measurements [13]. By using two probe pulses, this system can also generate up to three intermediate frequencies, which would provide more freedom in signal processing. Regardless of the frequency range of the system and the incoming vibrations, our method can suppress LSFD for either very high or very low vibration frequencies.

## 2. Theory

In the Φ-OTDR setup shown in Fig. 1, the light is split into the probe light and the local oscillator. The probe light shapes the pulse with a modulator and injects it into the FUT. The RBS and the local oscillator later beat together and create the intermediate frequencies.

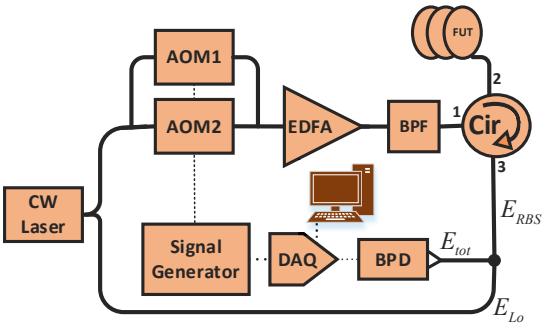


**Fig. 1.** Schematic of a heterodyne Φ-OTDR. CW Laser: continuous wave laser; AOM: Acousto-optical modulator; EDFA: erbium-doped fiber amplifier; BPF: bandpass filter; Cir: circulator; FUT: fiber under test; BPD: balanced photo detector; DAQ: data acquisition card.

When the angular frequency and electric field of the laser are $\omega_0$ and $E_{\mathrm{LO}} \cdot e^{(j(\omega_0+\omega_{drift}(t))t)}$, respectively; the backscattered electric field, which is shifted to $\omega_0 + \Delta\omega$ by the modulator, can be expressed as [14]

$$E_{RBS}(t) = \varepsilon_b . e^{\{j[(\omega_0+\Delta\omega+\omega_{drift}(t))t+\Phi(t)]\}} \tag{1}$$

where $\varepsilon_b$ and $\Phi(t)$ are the amplitude and phase of the backscattered signal, respectively. $\omega_{drift}(t)$ is a random function of the central frequency drift in the light source, which slowly changes with time. After $E_{\mathrm{LO}} \cdot e^{(j(\omega_0+\omega_{drift}(t))t)}$ beating with $E_{RBS}(t)$ we can extract a signal with frequency of $\Delta\omega + \omega_{drift}(t)$ by using a heterodyne detector.

If we shape two synchronized pulses wherein the second pulse has a constant delay of $\tau_d$, with the same light source as in Fig. 2 we will have

$$E_{RBS}(t) = k\varepsilon_b(e^{\{j[(\omega_0+\Delta\omega_1+\omega_{drift}(t))t+\Phi_1(t)]\}} + e^{\{j[(\omega_0+\Delta\omega_2+\omega_{drift}(t))t+\Phi_2(t)]\}}), \tag{2}$$

where $k$ is a constant and $\Delta\omega_1$ and $\Delta\omega_2$ are the up-shifting frequencies of the acousto-optical modulators (AOMs). We placed $k$ in Eq. (2) to emphasize the total amplitude could be something

Optics EXPRESS

higher than the aggregation of amplitudes in each single frequency. Since in a system with multiple probe frequencies, each single pulse would beat with other pulses in a pulse-train, and this could be also effective in the final amplitude.

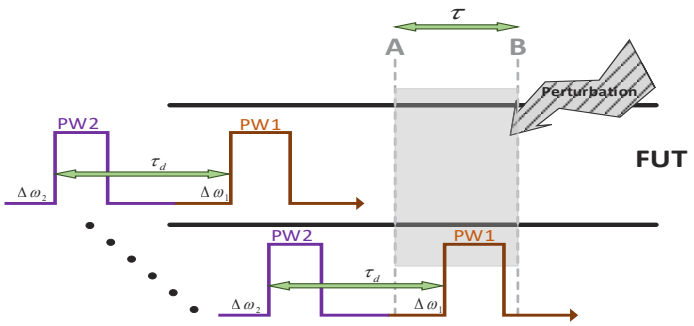


**Fig. 2.** Arrangement of the two pulses.

After beating $E_{RBS}$ and $E_{LO}$ (the electric field of the local oscillator) we get the heterodyne signal with two intermediate frequencies (IF). These two signals with different IF can be written as

$$i_1(t) = R_d\{2E_{LO}\varepsilon_b e^{j(\Delta\omega_1 t+(t\omega_{drift}(t)+\Phi_1(t)))}\} \tag{3}$$

and

$$i_2(t) = R_d\{2E_{LO}\varepsilon_b e^{j(\Delta\omega_2 t+(t\omega_{drift}(t)+\Phi_2(t)))}\}. \tag{4}$$

where $R_d$ is the responsivity of the photodetector. Then, $\Phi_1$ and $\Phi_2$ at any position can be extracted as

$$\Phi_1(t) = -j\ln\left(\frac{i_1(t)}{2R_dE_{LO}\varepsilon_b}\right) - \Delta\omega_1 t - t\omega_{drift}(t) \tag{5}$$

and

$$\Phi_2(t) = -j\ln\left(\frac{i_2(t)}{2R_dE_{LO}\varepsilon_b}\right) - \Delta\omega_2 t - t\omega_{drift}(t). \tag{6}$$

We always measure the change in phase between two given points. Th area between these two points is mostly referred as a gauge. If we consider the temporal distance between locations A and B (i.e. gauge) in Fig. 2 equal to $\tau$, for each IF we will have

$$\Delta\Phi_1 = \Phi_1(t) - \Phi_1(t+\tau) = -j\ln\left[\frac{i_1(t)}{i_1(t+\tau)}\right] + \Delta\omega_1\tau - t(\omega_{drift}(t) - \omega_{drift}(t+\tau)) \tag{7}$$

and

$$\Delta\Phi_2 = \Phi_2(t) - \Phi_2(t+\tau) = -j\ln\left[\frac{i_2(t)}{i_2(t+\tau)}\right] + \Delta\omega_2\tau - t(\omega_{drift}(t) - \omega_{drift}(t+\tau)). \tag{8}$$

If we set the time delay between pulses ($\tau_d$) to be big enough to satisfy the equations

$$\begin{matrix}\tau_d > \tau + PW_1 \\ \tau_d > \tau + PW_2\end{matrix}, \tag{9}$$

where $PW_1$ and $PW_2$ are the temporal pulse widths of $\Delta\omega_1$ and $\Delta\omega_2$, respectively. We can keep at least one pulse out of the gauge at any time. Therefore, when one frequency sweeps the gauge, the other is in the vicinity of but out of the gauge.

Optics EXPRESS

As mentioned earlier, $\omega_{drift}(t)$ is a slow-changing signal. We should also set $\tau_d$ to a value much lower than the period of changes in $\omega_{drift}(t)$, i.e., higher than the frequency content of $\omega_{drift}(t)$:

$$\hat{\omega}_{drift}(\xi) \ll \frac{1}{\tau_d} \tag{10}$$

where $\hat{\omega}_{drift}(\xi)$ represents the Fourier transform of the frequency drift signal. If, for example, the highest frequency in $\hat{\omega}_{drift}(\xi)$ is being considered as 10 Hz, all $\tau_d$ values under 0.001 second can meet the requirements for Eq. (10).

With Eqs. (9) and (10), there are two pulses: one making an RBS signal with both perturbation information and LSFD, and the other is in the vicinity of and containing LSFD data without perturbation information. Using this arrangement, we can remove terms $\omega_{drift}(t) - \omega_{drift}(t+\tau)$ in Eqs. (7) and (8) by subtracting them.

$$[\Phi_1(t) - \Phi_2(t)] - [\Phi_1(t+\tau) - \Phi_2(t+\tau)] = -j \ln\left(\frac{i_1(t) i_2(t+\tau)}{i_1(t+\tau) i_2(t)}\right) + \tau(\Delta\omega_1 - \Delta\omega_2). \tag{11}$$

Equation (11) suggests that by subtracting the left sides of the gauge containing each RBS signal from each other and right sides from each other, the effect of LSFD will be suppressed with good approximation. In other words, the second probe frequency can always be considered as a reference for the first probe and vice versa.

By unwrapping the radian phase angles in the right side of equations (11), we can get the phase change extracted almost without any effect of the frequency drift. Whenever the difference between consecutive angles is greater than or equal to $\pi$ radians, we shift the angles by adding multiples of $\pm 2\pi$ until the jump is less than $\pi$. In the areas where the signal-to-noise ratio (SNR) is low, we would face fading phenomenon [13]. We can predict occurrence of fading by finding the low-amplitude areas after multiplication of columns A and B. The multiplication of columns A and B is called the gauge-amplitude. In such cases the output phase will suffer from sudden jumps that should not be confused with LSFD. Figure 3 shows the phase output of a non-vibrated isolated fiber for 30 s. The fading areas are illustrated by red circles and the corresponding phase signal jumps abruptly. The decline in the phase (purple lines) is caused by LSFD. There are techniques to avoid phase jumps, such as using multiple probe frequencies [13] and change point detection (CPD) [10,15,16]. However, in this paper we only focus on the variations caused by LSFD.

It should be noted that these various probe frequencies must be properly selected to have the minimum possible phase correlation [17]. To remove the phase correlation between every two frequencies and to have independent probe lights, different frequencies must satisfy:

$$\Delta f = f_2 - f_1 \geq v_g/4L, \tag{12}$$

where $f_1$ and $f_2$ are the frequencies of the probe light, $v_g$ is the group velocity in the fiber, and $L$ is the physical distance between points A and B.

Optics EXPRESS

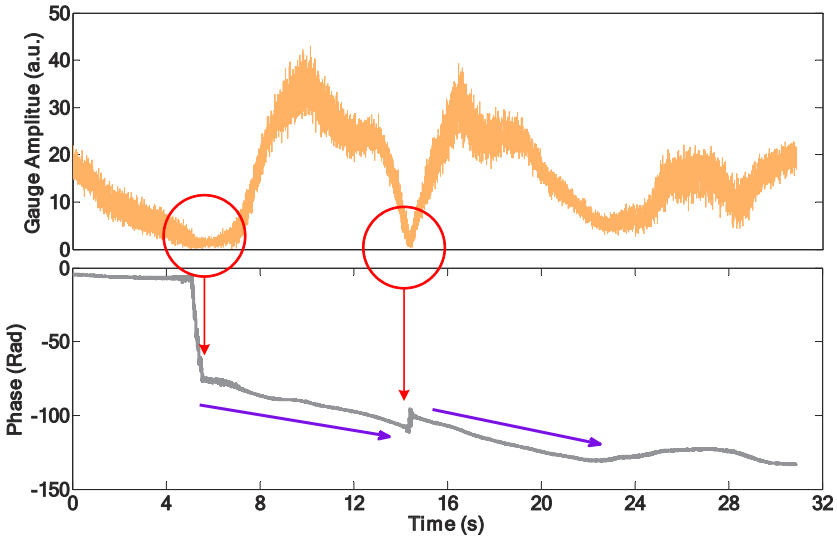


**Fig. 3.** Illustration of phase jumps and LSFD low frequency noise

## 3. Experimental results

We created a heterodyne Φ-OTDR setup like that illustrated in Fig. 1. A CW laser with frequency $\omega_0$ (1550 nm, RIO ORION laser module, 15KHz linewidth) is split into a local oscillator and sensing arm. The probe light pulses are shaped by two modulators with a 500-ns time delay. The first AOM makes a pulse with a 70-ns pulse width (PW1) and 100 MHz upshifting frequency. The second AOM creates a different pulse with a 100-ns pulse width (PW2) and 150 MHz upshift. The second pulse is injected 500-ns after the first. The pulse arrangement is shown in Fig. 2. These two pulses have a 500-Hz synchronized repetition rate. After amplification in an erbium-doped fiber amplifier, the probe pulses are launched into the FUT through a circulator. The first piece of fiber is 5000-m long and followed by a 15-m fiber wound around a cylindrical piezo electric (PZT) actuator, which was stimulated with a 1-Hz sinusoidal wave to be sufficiently similar to seismic moves and sub-Hertz vibrations. Then, a 200-m fiber is placed on the far end of the FUT and after the PZT. The RBS returning from the FUT at frequencies $\omega_0 + \Delta\omega_1$ and $\omega_0 + \Delta\omega_2$ are combined with the optical local oscillator and create intermediate frequencies $\Delta\omega_1$ and $\Delta\omega_2$. A balanced photodetector with 200-MHz bandwidth converts the optical signal to an electrical signal. An acquisition system is used to capture the data with a 500-MHz sampling rate.

In this experiment we consider PW1 as the main signal sweeping the gauge and PW2 as the reference signal for LSFD compensation. When we are mapping the results from two pulses on a same location axis to first find the vibration location, the one which triggered later will be shifted a little bit to the right, as showed in Fig. 4. In other words, when PW1 sees both vibration and LSFD, the PW2 sees only LSFD which is highly similar to the LSFD from PW1. Therefore, we can remove the LSFD from them both figures based on Equations (11).

We consider a 30-m gauge, placed between 4986-m and 5016-m locations of the FUT. As Fig. 5 shows, the reference signal itself would suffer from phase jump in the fading area. Therefore, we first correct the signal using a regression compensation CPD method [18]. After compensating the jumps in the reference signal, which appear during unwrapping in the fading areas, we can directly use the reference signal for LSFD compensation. Figure 6 illustrates the approach suggesting by Eq. (14). In Fig. 6 the 1-Hz vibration was successfully captured by the interrogator (orange plot, Eq. (7)), but an unexpected downward trend is observed. This trend could be from

Optics EXPRESS

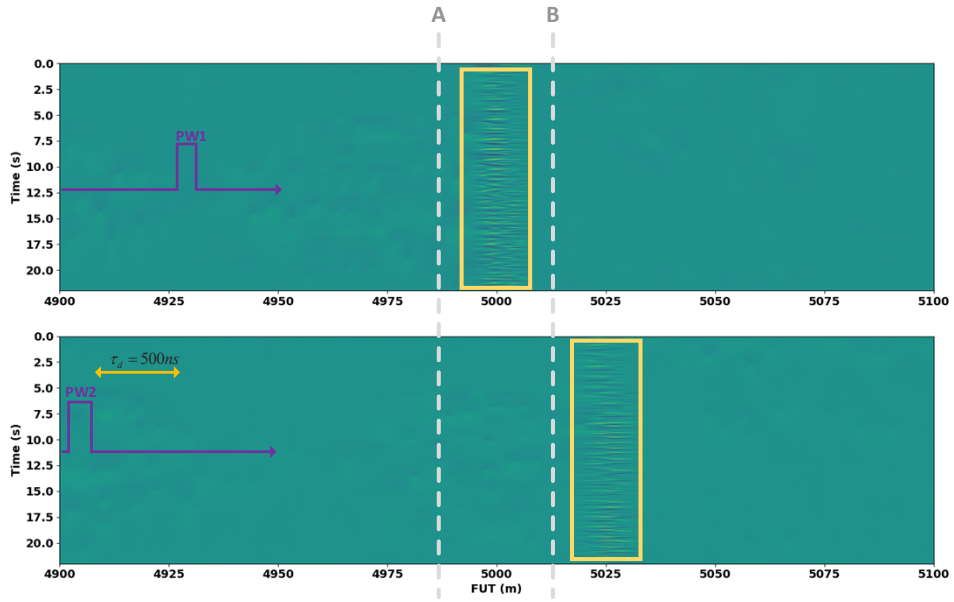


**Fig. 4.** Plotting RBS from both signals on the same spatial axis

an external source or LSFD; however, it also exists in our reference signal (blue plot, Eq. (8)). Therefore, we can mathematically counteract these two plots to distinguish them from LSFD or other low frequency noise.

It should be noted that in many mathematical algorithms and automated measuring devices, sub-Hertz frequencies would be suppressed regardless if they are noise or informative signal. For example, in measuring the power spectral density (PSD), the amplitude is normalized by the frequency resolution and consequently vanishes near zero frequencies. Signal smoothing techniques are another common method used in many commercial devices and they sometimes remove high-power low frequencies with detrending methods [19], which could also result in missing some information in the near zero band. However, using a reference signal is also helpful to analyze PSD and the frequency domain with minimum loss of meaningful data. Figure 7 represents the vibration signal, reference signal, and the compensated signal in the frequency domain. The 1-Hz vibration is clearly observed by the compensated signal and the SNR of the signal before and after compensation remain the same. This promisingly shows that no power loss occurred during the compensation. Also, the DC offset was removed and the low frequencies mainly caused by LSFD were suppressed while the vibration signal remained and was purified.

In another attempt, we used a system as described above without external vibration. We randomly selected four time periods and performed the proposed compensation method. The capturing time (1200 ms) was sufficient to see the influence of sub-Hertz changes. As Fig. 8 shows, the compensated phase signal was acceptably free of LSFD and was flattened, as expected.

When we measure the strain change for example, an upward trend through the time shows stretch and a downward trend represents compression. In Fig. 8 the two above plots can be easily misunderstood with a stretch in the FUT, and the two bottom plots with a compression. While using the proposed method cleared that no physical stretch and compression happened, as we planned the experiment without any mechanical perturbation.

Optics EXPRESS

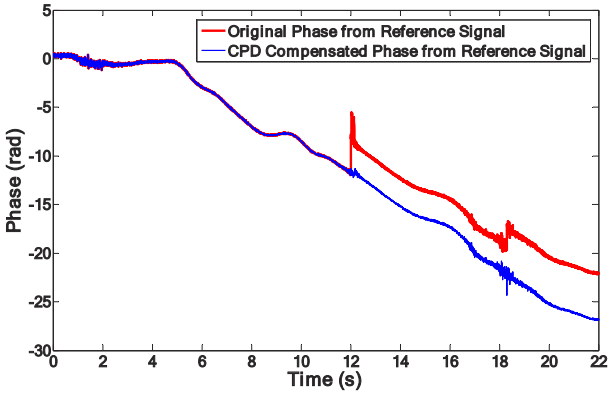


**Fig. 5.** Initial phase correction in jump points of the reference signal.

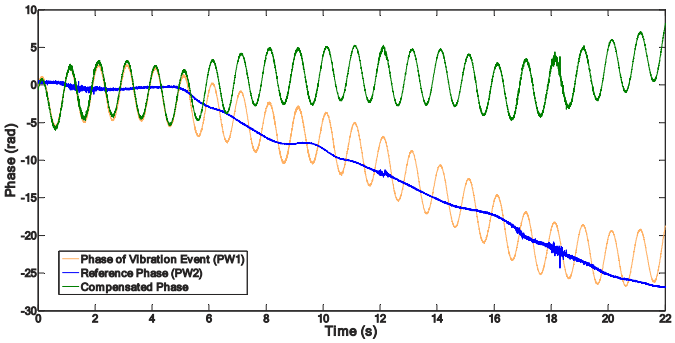


**Fig. 6.** Purification of signal from low frequency noise by counteracting phase and reference signals.

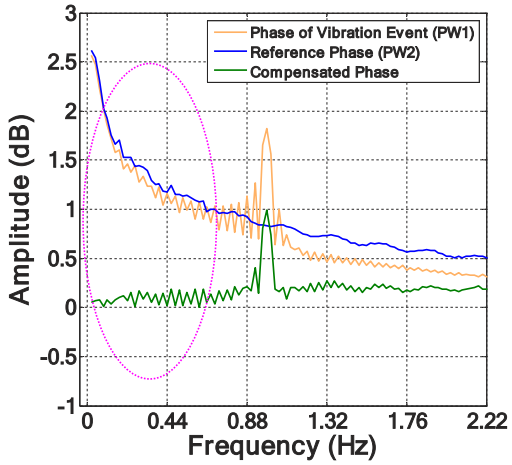


**Fig. 7.** Performance of compensation with a reference signal in the frequency domain.

Optics EXPRESS

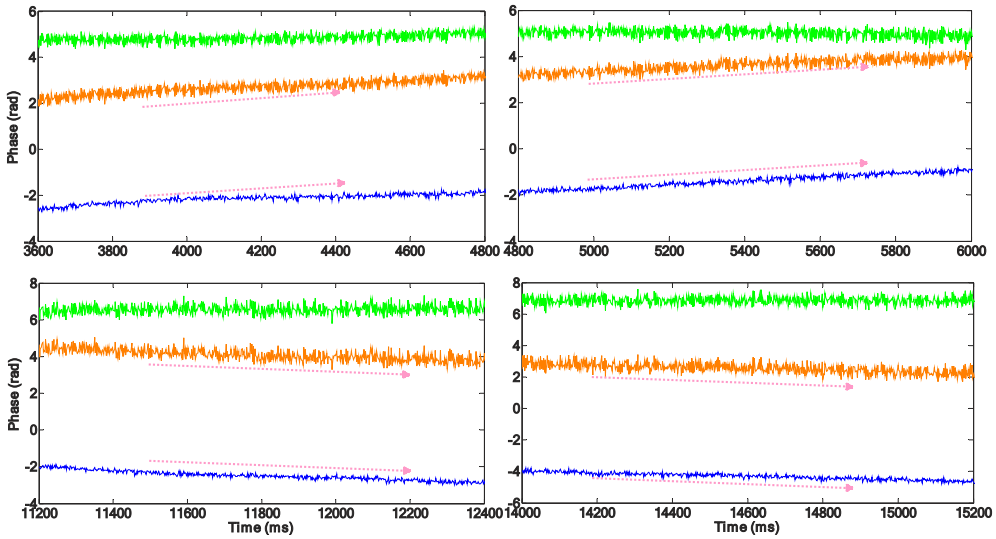


**Fig. 8.** Four randomly captured data frames. The orange, blue, and green plots are the main, reference, and compensated signals, respectively. Pink arrows show the upward/downward trends in the main and reference plots, which are compensated in the final output.

## 4. Conclusion

In this study, an approach for mitigation of LSFD in Φ-OTDR systems was proposed. By using one probe pulse as a reference in a system with two or more probe frequencies, we can remove unwanted low frequency noise that is originally caused by the laser source. Although LSFD is problematic issue, it is not the only source of low frequency noise. Change in temperature, humidity, physical surroundings, environment, etc., can result in such noises. The proposed method; however, is expected to highly suppresses all of these effects, regardless of their source, either in the time or frequency domain.

For comparing reference and probe signals, there are sophisticated methods, rather than normal differentiation, available for use. Some of these methods have a close relationship with CPD methods and can further enhance the results. These methods can be further discussed in an independent research or future work.

The proposed method is very helpful for increasing accuracy in passive and active seismic monitoring, reservoir monitoring, underwater monitoring, etc. It also helps using relatively simpler laser sources and make the whole system price-efficient, as well as processing data without lengthy compensation algorithms.

**Funding.** Federal Ministry for Economic Affairs and Climate Action (FKZ: 03EE4009B).

**Acknowledgments.** This research was carried out in the framework of the research project "Distributed fiber optic strain sensing along existing telecommunication networks for efficient seismic exploration and monitoring of geothermal reservoirs" (project acronym SENSE). It was supported by the Federal Ministry for Economic Affairs and Climate Action, FKZ: 03EE4009B. The authors thank for the financial support and all the partners of the project consortium for helpful discussions. We also thank Sven Münzenberger from BAM for his technical supports.

**Disclosures.** The authors declare no conflicts of interest.

**Data availability.** Data underlying the results presented in this paper are not publicly available at this time but may be obtained from the authors upon reasonable request.

## References

1. N. Guo, L. Wang, H. Wu, C. Jin, H.-Y. Tam, and C. Lu, "Enhanced coherent BOTDA system without trace averaging," J. Lightwave Technol. **36**(4), 871–878 (2018).

Optics EXPRESS


2. F. Wang, X. Zhang, X. Wang, and H. Chen, "Distributed fiber strain and vibration sensor based on Brillouin optical time-domain reflectometry and polarization optical time-domain reflectometry," Opt. Lett. **38**(14), 2437–2439 (2013).
3. Q. Cui, S. Pamukcu, W. Xiao, and M. Pervizpour, "Truly distributed fiber vibration sensor using pulse base BOTDA with wide dynamic range," IEEE Photonics Technol. Lett. **23**(24), 1887–1889 (2011).
4. D. Zhou, Y. Dong, B. Wang, C. Pang, D. Ba, H. Zhang, Z. Lu, H. Li, and X. Bao, "Single-shot BOTDA based on an optical chirp chain probe wave for distributed ultrafast measurement," Light: Sci. Appl. **7**(1), 32 (2018).
5. F. Wang, Y. Zhang, W. Wang, R. Dou, J. Lu, W. Xu, and X. Zhang, "Development of a multiperimeter sensing system based on POTDR," IEEE Photonics J. **10**(3), 1–7 (2018).
6. M. Zabihi, X. Chen, T. Zhou, J. Liu, F. Wang, Y. Zhang, and X. Zhang, "Compensation of optical path difference in heterodyne Φ-OTDR systems and SNR enhancement by generating multiple beat signals," Opt. Express **27**(20), 27488–27499 (2019).
7. F. Zhu, X. Zhang, L. Xia, Z. Guo, and Y. Zhang, "Active Compensation Method for Light Source Frequency Drifting in Φ-OTDR Sensing System," IEEE Photonics Technol. Lett. **27**(24), 2523–2526 (2015).
8. Z. Pan, K. Liang, Q. Ye, H. Cai, R. Qu, and Z. Fang, "Phase-sensitive OTDR system based on digital coherent detection," in *Asia Communications and Photonics Conference and Exhibition*(Optical Society of America2011), p. 83110S.
9. Q. Yuan, F. Wang, T. Liu, Y. Zhang, and X. Zhang, "Using an auxiliary Mach–Zehnder interferometer to compensate for the influence of laser-frequency-drift in Φ-OTDR," IEEE Photonics J. **27**(3), 3664 (2019).
10. X. Lu and K. Krebber, "Phase error analysis and unwrapping error suppression in phase-sensitive optical time domain reflectometry," Opt. Express **30**(5), 6934–6948 (2022).
11. Q. Yuan, F. Wang, T. Liu, Y. Liu, Y. Zhang, Z. Zhong, and X. Zhang, "Compensating for influence of laser-frequency-drift in phase-sensitive OTDR with twice differential method," Opt. Express **27**(3), 3664–3671 (2019).
12. R. Zhao, H. Yuan, B. Jin, Y. Xu, Y. Chen, X. Liu, Q. Bai, and Y. Wang, "Frequency drift mitigation of Φ-OTDR using difference-fitting method," Appl. Opt. **60**(2), 459–464 (2021).
13. M. Zabihi, Y. Chen, T. Zhou, J. Liu, Y. Shan, Z. Meng, F. Wang, Y. Zhang, X. Zhang, and M. Chen, "Continuous fading suppression method for Φ-OTDR systems using optimum tracking over multiple probe frequencies," J. Lightwave Technol. **37**(14), 3602–3610 (2019).
14. A. H. Hartog, *An introduction to distributed optical fibre sensors* (CRC press, 2017).
15. R. Corradin, L. Danese, and A. Ongaro, "Bayesian nonparametric change point detection for multivariate time series with missing observations," Int. J. Approximate Reasoning **143**, 26–43 (2022).
16. X. Ge and A. Lin, "Kernel change point detection based on convergent cross mapping," Commun. Nonlinear Sci. Numerical Simulation **109**, 106318 (2022).
17. K. Shimizu, T. Horiguchi, and Y. Koyamada, "Characteristics and reduction of coherent fading noise in Rayleigh backscattering measurement for optical fibers and components," J. Lightwave Technol. **10**(7), 982–987 (1992).
18. C. Truong, L. Oudre, and N. Vayatis, "Selective review of offline change point detection methods," Signal Process. **167**, 107299 (2020).
19. E. S. Gardner, "Exponential smoothing: The state of the art—Part II," Int. J. Forecasting **22**(4), 637–666 (2006).